Chapter

3

Experimental Procedures and Evaluation of Different Parameters

Contents

3.1 Introduction

In view of the desired aims and objectives for the present study; various experimental techniques are needed to be utilized for the dielectric, physical and acoustical property characterization. For accurate and precise measurements, proper calibration method is followed to the apparatus as described in their corresponding user manual. In addition to this, experimental measurements of the dielectric properties (dielectric constant, dielectric loss), physical properties (density, viscosity and refractive index) and acoustical property (ultrasonic velocity) are also carried out and compared with the literature values, which has been also discussed in this chapter.

3.2 Materials and Sample Preparation

3.2.1 Material

In present study organic liquid for n-Hexanol, n-Octanol and N, N Dimethylformamide (DMF) of were obtained from Loba Chemi. Pvt Ltd, (India) respectively and used as received. Structure, Purity, Grade, CAS No and IUPAC name are tabulated in Table 3.1.

Table 3.1 The sources and grades, CAS No, IUPAC Name and purity of chemicals used in the present work.

Compound	n-Hexanol	n-Octanol	N, N-Dimethylformamide
Chemical Structure			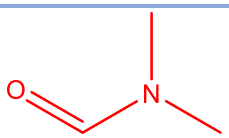
Purity	99.0 %	99.0 %	99.8 %
Grade	AR	Synthesis	AR
CAS No	111-27-3	111-87-5	68-12-2
IUPAC Name	hexan-1-ol	octan-1-ol	N, N-dimethylformamide

3.2.2 Sample preparation

Binary mixture of n-Hexanol with DMF and n-Octanol with DMF were meticulously prepared in hermetically sealed glass vials at different volume percentages (0,10, 20, … 100%) of DMF in n-Hexanol and n-Octanol. Under the assumption of perfect mixing, volume percentage may be converted into mole fraction using the following formula:

$$x_1 = \frac{\left(\frac{V_1\rho_1}{M_1}\right)}{\left(\frac{V_1\rho_1}{M_1}\right)+\left(\frac{V_2\rho_2}{M_2}\right)} \quad (3.1)$$

Where V_1 and V_2 are the volume percentage, ρ_1 and ρ_2 are the densities and M_1 and M_2 are the molecular weight, suffix '1' represent n-Hexanol or n-Octanol and suffix '2' represent DMF respectively.

The samples were securely sealed in borosilicate glass bottles to safeguard against atmospheric moisture. To maintain purity, all equipment and glassware underwent thorough cleaning with double distilled water and acetone prior to use, ensuring the reliability of experimental results.

3.3 Methods

The experimental techniques utilized in this study involved precise measurements of dielectric constant, density, refractive index, ultrasonic velocity, and viscosity. The accuracy of these measurements depends not only on instrument precision but also on substance purity. All chemicals used were analytical grade (AR) with a minimum assay purity of 99.0% from Loba Chemi Pvt Ltd, India. Purity was confirmed by measuring refractive indices. Impurities can significantly alter substance behavior, underscoring the importance of using high-purity chemicals for reliable experimental data. Experimental methods used to measure these parameters are also described in this chapter.

The experimental part of the current study encompasses the determination of various properties for the liquid mixtures under investigation.

1.Measurement of complex permittivity ε*(f) in the frequency range of 20 Hz to 2 MHz using Precision LCR meter

2. Measurement of complex permittivity ε*(f) in the frequency range of 200 MHz to 20 GHz using VNA (Vector Network Analyzer)

3. Measurement of refractive index (n)

4. Measurement of density (ρ)

5. Measurement of ultrasonic velocity (U)

6. Measurement of viscosity (η)

3.3.1 Measurement of complex permittivity ε*(f) in the frequency range of 20 Hz to 2 MHz using Precision LCR meter

Using a precision LCR meter (Agilent E-4980A), the complex dielectric permittivity ε*(f) of DMF solutions in various solvents (n-Hexanol and n-Octanol) was determined

through capacitance (Cp) and resistance (Rp) measurements across a frequency spectrum spanning from 20 Hz to 2 MHz, encompassing 201 frequency points on a logarithmic scale. Capacitance and resistance with and without liquid were measured using a four-terminal liquid dielectric test fixture (Agilent 16452 A) (Fig.3.1). During the calculation of the frequency dependent values of the complex dielectric function, the short circuit compensation of the cell and its correction coefficient were evaluated to eliminate the effect of stray capacitance.[1]

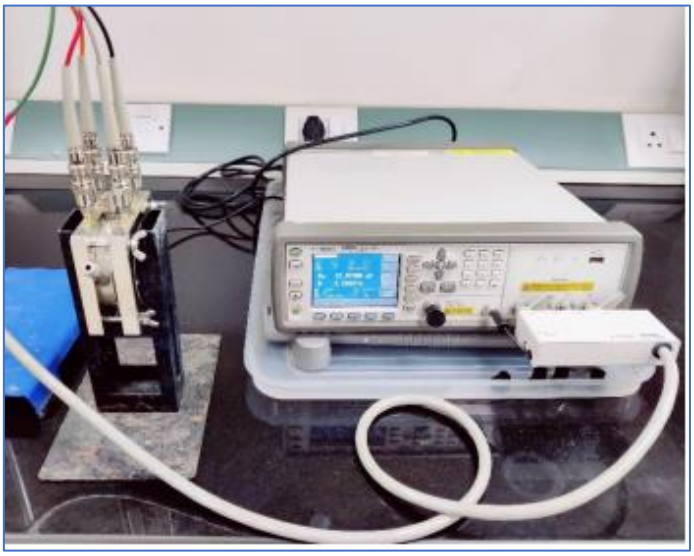

Fig. 3.1 Complex permittivity measurement by Precision LCR meter (Agilent E4980A) with four terminal liquid test fixture (Agilent 16452A**)**.

Fig. 3.2 Constant temperature water bath (Model Industrial Corporation).

The experimental method for determining complex dielectric permittivity spectra, as well as its measurement accuracy, is discussed in the stated references [1,2]. The accuracy of the determined complex dielectric permittivity is 0.3%. Measurements of the dielectric permittivity spectra were taken at the three different temperatures starting from 293.15 and ending with 313.15 K in the interval of 10 K. A thermostat (MIC

Fourtech; India) was used to maintain the temperature, which is having a standard accuracy of ± 0.1K (Fig.3.2).

The complex dielectric function ε*(f) was derived from the precise measurements of parallel capacitance (Cp) and parallel resistance (Rp) using the given equation.

$$\varepsilon^*(f) = \varepsilon' - j\varepsilon'' = \alpha\left(\frac{C_P}{C_0} - j\frac{1}{\omega C_0 R_P}\right) \quad (3.2)$$

In equation (3.2), the real a part of the complex permittivity is a measure of the electrical energy storage capabilities of the dielectric material, and the imaginary part indicates an average energy loss per cycle due to the joules heating effect, ω = 2πf is the angular frequency, α is the correction coefficients of the cell, Cp is the capacitance of the test fixtures with sample, C_0 is the capacitance of the test fixture without sample, and Rp is the parallel resistance of the test fixtures with sample. The LCR meter was calibrated prior to initiate the experiment using the procedure described in the User's manual. [3]. Experimental setup for Precision LCR meter (Agilent E4980A) with four terminal liquid test fixture (Agilent 16452A**)** is connected to the laptop is depicted in Fig. 3.3.

Fig. 3.3 Experimental setup for Precision LCR meter (Agilent E4980A) connected four terminal liquid test fixtures (Agilent 16452A) with constant temperature water bath.

3.3.2 Measurement of complex permittivity ε*(f) in the frequency range of 200 MHz to 20 GHz using VNA (Vector Network Analyzer)

In the microwave frequency range, we can measure the complex permittivity ε*(f) of a sample using either time domain or frequency domain methods. Let's focus on the frequency domain approach using a Vector Network Analyzer (VNA). VNA is made up of a signal source, receiver, and display. During measurement, the source emits a signal towards the material under test (MUT) at a specific frequency, while the receiver is adjusted to that frequency to capture reflected and transmitted signals from the material.

The measured response reveals the magnitude and phase of the reflected and transmitted signals at that frequency. This process is repeated across various frequencies, showcasing the reflection and transmission measurement responses as a function of frequency. To illustrate, Fig. 3.4 provides a typical setup for measuring liquid materials using a semi-rigid coaxial probe and a VNA. This probe, equipped with a connector, connects to the VNA to analyze the complex dielectric permittivity of liquid samples. During the measurement, we dip the opposite end of the semi-rigid coaxial probe into the liquid, and the VNA measures the probe's reflection coefficient.

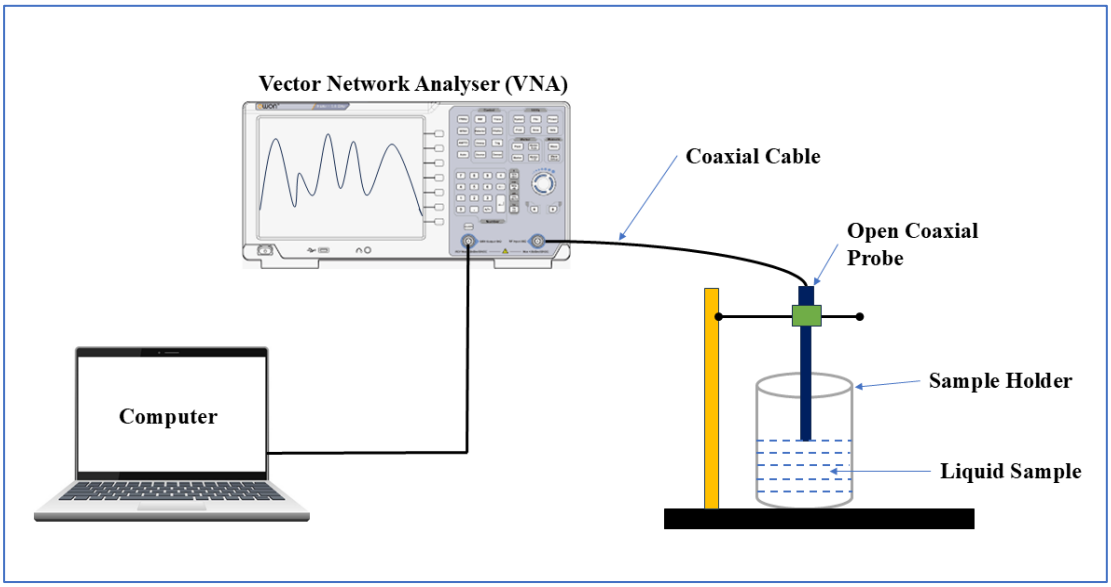

Fig. 3.4 Schematic diagram of vector network analyzer (VNA) measurement set up with co-axial probe.

The Anritsu Shock line MS46322A series vector network analyzer (VNA) shown in Figure 3.5 was utilized to conduct dielectric measurements on liquid samples (n-Hexanol, n-Octanol with DMF). These measurements spanned a frequency range from 200 MHz to 20 GHz and a temperature range from 293.15 K to 313.15 K, with intervals of 10 K and a precision of ± 0.1 K. Using a DAK-3.5 probe, as depicted in Figure 3.6, facilitated these measurements, operating within the frequency range of 200 MHz to 20 GHz. Detailed characteristics, dimensions, and materials of the DAK-3.5 probe can be found in Table 3.2.

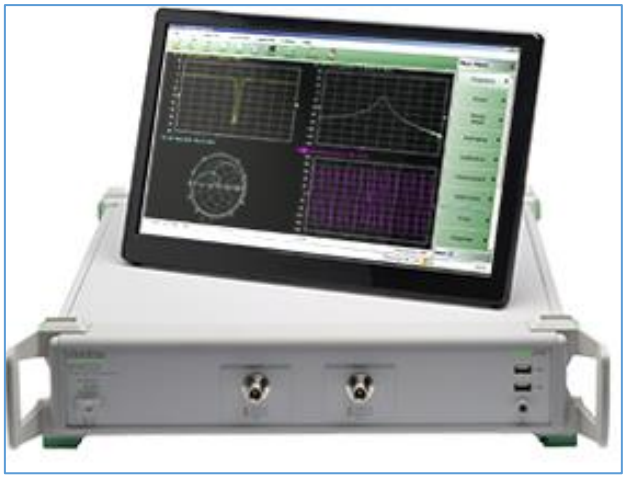

Fig. 3.5 Anritsu Shock line Vector Network Analyzer (VNA) MS46322A.

Fig. 3.6 SPEAG DAK-3.5 Probe.

To control the VNA remotely and measure the dielectric constant and dielectric loss, SPEAG DAK software v2.1.144 was utilized. This software offers precise measurements of dielectric parameters for liquids, solids, and semi-solids. It features advanced computations for quick and accurate estimations, enhanced visualization, and extensible scripting capabilities. VNA programming is accomplished remotely over LAN communications in conjunction with SPEAG DAK (Dielectric Assessment Kit) (Fig.3.7).

Fig. 3.7 SPEAG Dielectric Assessment Kit (DAK).

Table 3.2 Specifications of DAK-3.5 probe.

Title	Specification
Frequency range	200 MHz to 20 GHz
Dielectric bead material	Stycast ^{TM} (ε'=2.538)
Diameter of dielectric bead	12 mm
Diameter of flange	48 mm
Impedance	50 Ω
Operating temperature	0-60° C
Connector type (male)	3.5 mm

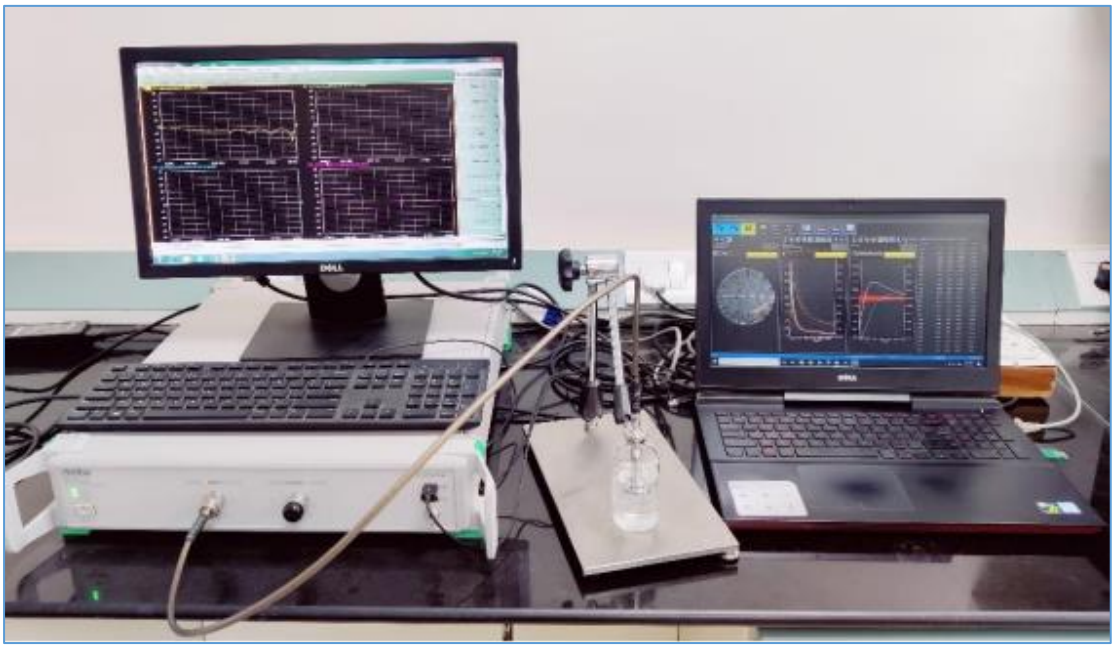

Fig. 3.8 Experimental setup of Anritsu Shockline VNA MS46322A along with SPEAG DAK.

The practical setup of the Anritsu Shockline VNA MS46322A and the dielectric probe (SPEAG DAK-3.5), along with the liquid material, is illustrated in Figure 3.8. The probe is connected to the VNA via a coaxial cable to measure the complex reflection coefficient, S11, at the probe end. This measured reflection coefficient is then converted to the complex permittivity of the material under test. To perform dielectric measurements of the liquid material accurately, a specific procedure is followed, as outlined in reference [4]. Calibration is a crucial step in this process, which involves normalizing the magnitude and phase changes of the probe and cable. This ensures that the reflection coefficient measurement by the VNA is referenced to the probe's flange.

The precision of dielectric measurements relies on the accuracy of this calibration process. The DAK framework is adjusted using SPEAG's high-quality standards (Open, Short, and Load) to achieve this calibration, as detailed in references [4,5].

1. Open measurement

To perform the open circuit/open measurement, the dielectric probe is kept in the air, and then the 'open' button in the DAK software calibration section is clicked. This action records the open circuit measurement and applies a calibration factor to it. Because of the radiation of fields from the probe into the air, the true open circuit (where ZL is less than infinity) at the probe interface differs from the ideal open circuit (where ZL equals infinity). The DAK software calculates and compensates for the true open circuit at the probe's flange contact during calibration. Confirmation of the open measurement is indicated by a small dot on the right side of the Smith chart, as depicted in schematic Fig. 3.9. This dot confirms that the measurement accurately represents real-world conditions, accounting for any deviations from ideal scenarios.

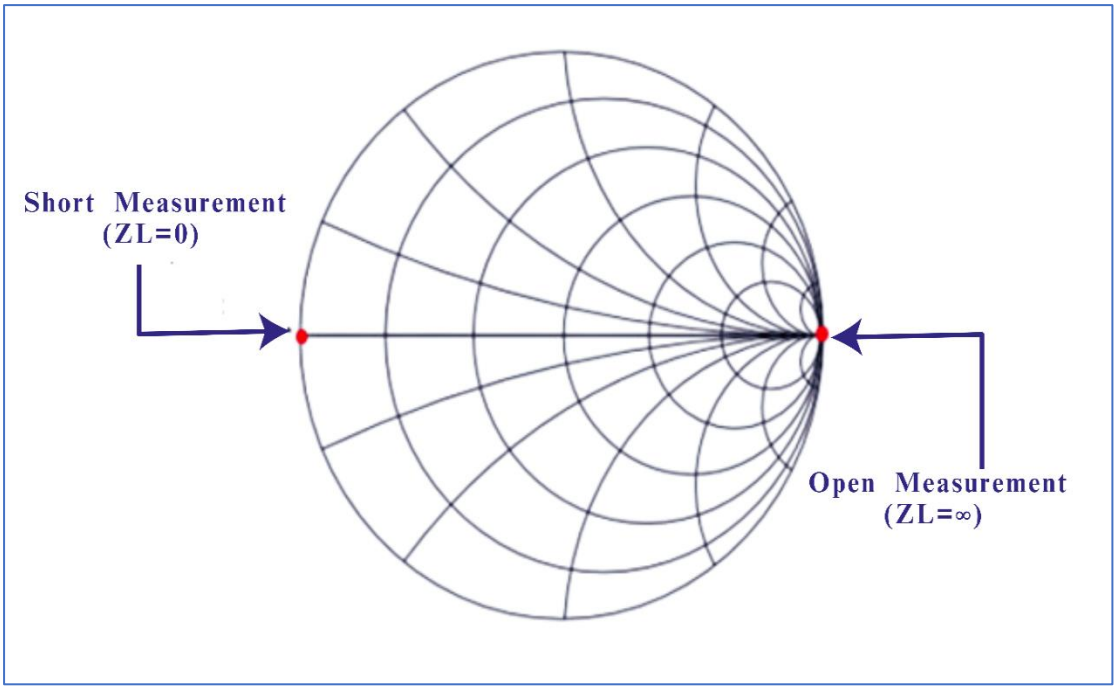

Fig. 3.9 Schematic diagram of Smith chart showing open and short measurements.

2. Short Measurement

In the calibration process, it's crucial to get accurate short circuit measurements. To achieve this, we use a highly conductive copper strip, as seen in Figure 3.10. Before using it, we make sure the surface is clean by using sandpaper to remove any oxides, and then we clean it with methanol. This ensures good electrical contact between the

probe and the copper strip, which is essential for precise short measurements. To ensure consistent and reliable contact between the copper strip and the flange of the dielectric probe, we use a high-quality shorting block, also shown in Figure 3.10. This block helps maintain excellent and consistent contact, improving the accuracy of the short circuit measurements during calibration.

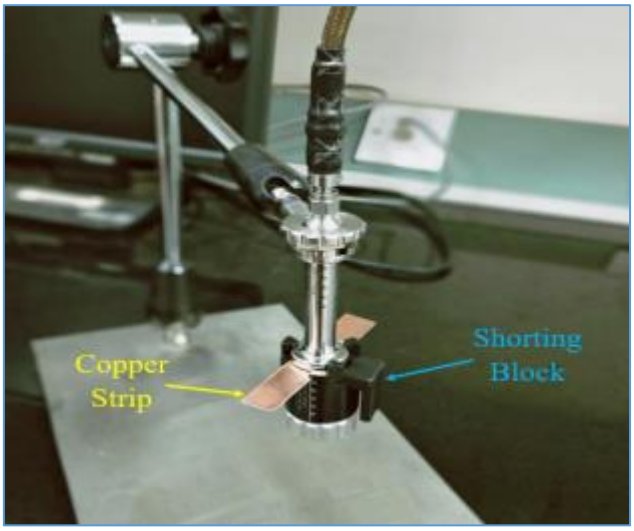

Fig. 3.10 Calibration set up for short measurement showing copper strip and shorting block.

Following the short measurement setup illustrated in Figure 3.10, the short circuit measurement was conducted by clicking the 'Short' button in the calibration section of the DAK software. In an ideal situation where the impedance (Z) is zero, the quality of the short measurement was assessed by observing a small dot in the Smith chart. This dot should be positioned at the left end of the Smith chart, as depicted in Figure 3.9.[6] This dot serves as confirmation that the short circuit measurement accurately reflects the ideal scenario where impedance is minimal.

3. Load Measurement

To measure the dielectric load, the dielectric probe was dipped into a standard liquid material. Then, by clicking the 'Load' button in the DAK software, we measured the load. We checked the calibration by testing a standard liquid sample. Once we were happy with the results, we tested solutions of DMF with polar solvents (n-Hexanol and n-Octanol) using the same method.

We conducted a frequency sweep using the VNA through the DAK software and calculated the dielectric parameters like dielectric constant and loss from the VNA's results. This sweep covered frequencies from 200 MHz to 20 GHz for 397 frequency

points.[5] Throughout the tests, we kept the solutions at the right temperature using a constant temperature bath.

3.3.3 Measurement of Refractive Index (n)

This instrument measures the refractive index of liquids or solids. Refractive indices and mean dispersions are important optical constants of a substance and can be used to determine the optical performance, purity, concentration and dispersion etc. Therefore, the refractometer is an indispensable tool within a wide range of industries, such as pharmaceutical, chemical and sugar making industries, as well as in factories, colleges and in research institutes. This device measures the angle of refraction at liquid solid interface. The angle of refraction depends on the composition of liquid, which allows the use of refractometer for quick evolution of concentration of dissolved substance.

Fig.3.11 Abbe's Refractometer.

Principle

The abbe's refractometer is the most accurate and convenient instrument for determining the index of refraction. The measurement is based on the observation of

the refracted beam passing the substance to be measured and entering a standard prism of high refractive index at grazing incidence.

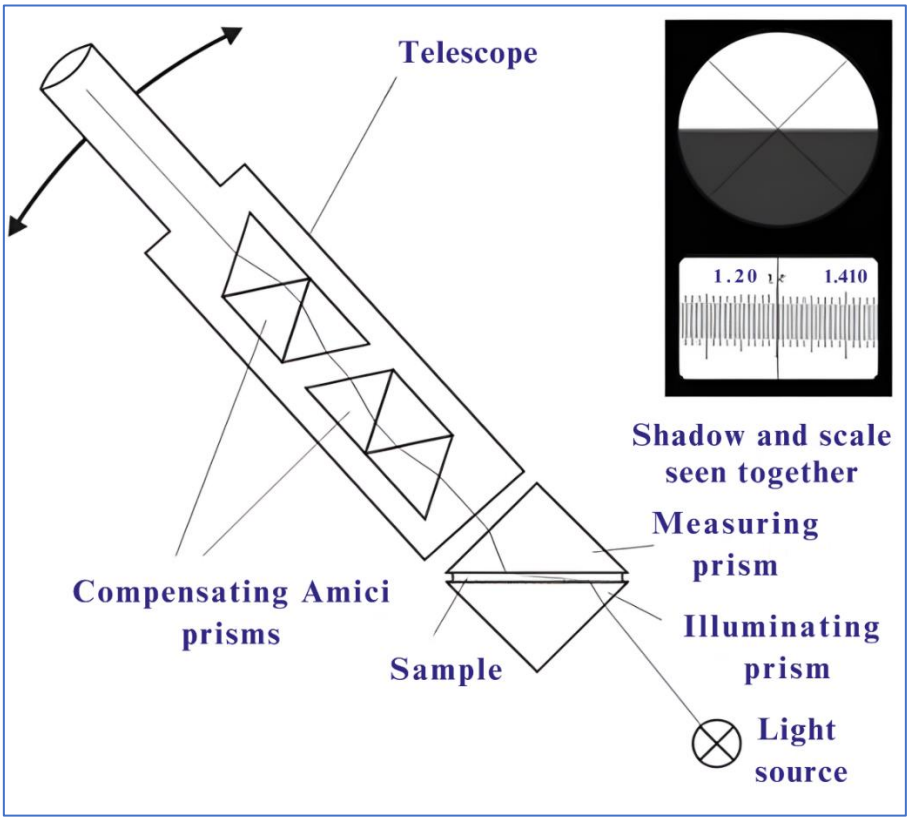

Fig.3.12 Internal structure of Abbe's Refractometer.

Consequently, the critical ray makes a boundary between a dark and light area. This is more 7clearly shown in fig 3.11. For monochromatic illumination this boundary will be a sharp up line. For measurement of the critical angle as commonly made in lab, as shown in fig 3.11, the circle of figure illustrates the appearance of the field of view of the observing telescope. This method is commonly used to measure the index of refraction of liquid by placing it in contact with the prism; it is of advantage to derive an expression to take the place upon the assumption that the incident beam, upon passing in to prism, passes from a medium of index. Under these circumstances, for grazing incident ray, I =90. In addition, r+r'=A. where A is the refracting angle of the prism. By eliminating r and r' from this equation we can get refractive index. This equation shows the refractive index n of the medium in contact with the prism for the condition of grazing incidence of the light (sodium D light (of wavelength 5890 Å)). For greater convenience of measurement, the refractometer built on this principle are equipped with the calibrated scale. The abbe's refractometer measures the refractive index in the range from 1.3 to 1.7 with the accuracy up to 0.0002. The essential feature

of this instrument is the use of Abbe's prism, two similar 45 degrees prisms of refractive index.

According to the law of conversion, n=sin(i)/sin(r), where i and r are incident and refracted ray. n is a constant called the index of refraction. From this equation, it is evident that when light is incident upon a transparent body, there will be definite angle of refraction corresponding to every angle of incidence. But the upper limit of the angle of incidence is 90 degrees. There will be a corresponding limit on angle of refraction which determines the largest angle which any ray penetrating the body may make with the normal. To an observer at 0, inside a medium of refractive index n, all rays incident upon the surface from above are confined, upon refraction, within a cone corresponding to the angles of refraction from zero up to critical angle. No illumination exists from any direction whose angle with the normal is greater than this critical angle.

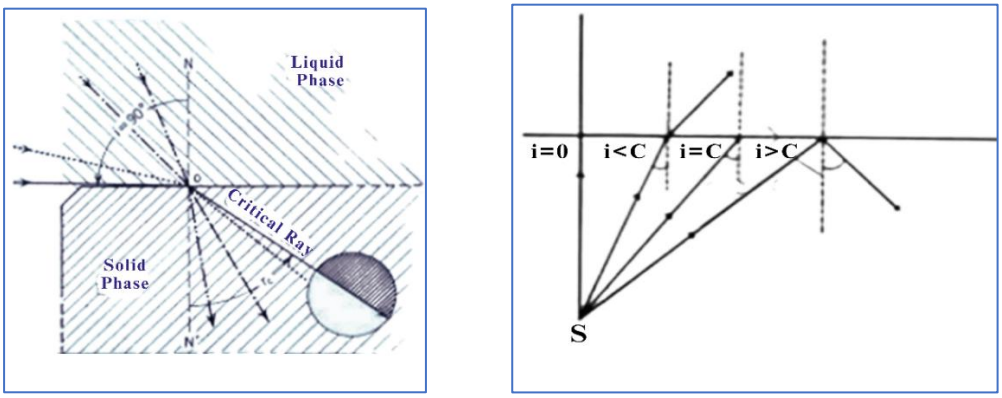

Fig.3.13 (A) critical angle and **(B)** Total internal reflection.

A drop of liquid whose index is desired is placed on the hypotenuse of one prism and hypotenuse of another prism is placed upon the first one. So that they form a cubical block 8 of glass. It is then evident that for slightly convergent or divergent light incident from the appropriate direction upon the junction of the two prisms, a part will be transmitted and a part will be totally reflected if the refractive index of liquid is less than that of the prism. A telescope focused for parallel light will show the characteristic divided field. The index of the liquid is then read directly from the calibrated scale. The calibration is made for sodium light, but the calibration can also be made using daylight illumination. This is made possible by using a compensator consisting of two direct vision prisms. They can be rotated in opposite direction at equal rates, and form together a system of dispersion. In this way the amount of dispersion can be introduced to counteract that of the specimen under examination. The compensator carries a scale by

means of which a measurement of the dispersion of the material under examination may be obtained.

Procedure:

(1) The scale and the cross hair are focused by turning the eyepiece.

(2) The illumination of the scale is adjusted by turning the small tube projecting at the lower end of the instrument.

(3) Turn the knob connected to prism to lift it up and apply the sample which is to be tested. After that lock the prism is into its rest position.

(4) Start the sodium lamp and adjust its position, open the reflecting mirror of the upper prism and adjust it for good illumination of the scale.

(5) Adjust the position of prism by turning the knob at the lower right until in the middle of the bright circle a clear boundary line is observed between a dark grey sector in the lower half and a bright sector in the upper half. Adjust the knob so that boundary line passes through the center of the cross-hair.

(6) Read off the index of refraction on the illumination scale directly up to the third decimal and estimate the value of fourth.

(7) Read and record the temperature of the thermometer attached to the instrument. Repeat the procedure with other samples, with different concentrations. The binary mixtures are composed of constituents belonging to different classes of compounds, various molecular interactions are present. In that sense, the applicability of mixing models are the most important mixing rules to the binary mixtures under consideration has been tested. The following relations are used for the prediction of refractive index in the binary liquid mixtures.

3.3.4 Measurement of Density (ρ)

Fig. 3.14 Specific gravity bottle for density (ρ) measurement.

Density plays a critical role in chemical materials and their processing, being influenced by temperature variations.[7] Accurate density measurement is vital for numerous applications, including fluid mechanics, mass transfer calculations, and the design of chemical processes.[8] To determine the density of both pure liquids and their mixtures, a 10 ml specific gravity bottle equipped with a capillary tube is commonly employed. This apparatus, as depicted in Fig. 3.14, facilitates precise measurements, ensuring reliable data for various engineering tasks. A specific gravity bottle is typically made of glass, with a tightly fitting ground glass stopper and a small tube to prevent air bubbles. The densities are measured with an accuracy of 0.1 kg m^{-3}. Here's a simplified explanation of the procedure used to determine the density of liquid mixtures. We used a glass bottle with a tight lid and a small tube to avoid air bubbles. We aimed to find the density of liquid mixtures accurately.

Procedure:

1. First, clean the specific gravity bottle meticulously using acetone and ensure it is completely dry.
2. Then, measure the weight of the empty specific gravity bottle, denoted as W_1 grams.
3. Fill the specific gravity bottle with distilled water up to the tip of the capillary point. Measure the weight of the specific gravity bottle filled with distilled water, denoted as W_2 grams. Ensure no air bubbles are trapped in the apparatus during filling.
4. Afterward, clean the specific gravity bottle again with acetone and ensure it is thoroughly dried.
5. Fill the specific gravity bottle with the liquid sample up to the tip of the capillary point. Measure the weight of the specific gravity bottle filled with the liquid sample, denoted as W_3 grams. Ensure no air bubbles are present in the apparatus during filling.
6. Remove the liquid sample from the specific gravity bottle and clean the bottle with acetone, ensuring thorough drying. Repeat the entire procedure for each subsequent sample.
7. Place the specific gravity bottle in a constant temperature water bath without any disturbance to its volume, ensuring that the temperature remains consistent throughout.

   In this way, using the following equation, liquid density can be calculated.

$$\rho = \rho d.w \frac{(Wl - We.b.)}{(Wd.w. - We.b)} \quad (3.3)$$

Where ρ is the Density of liquid and $\rho_{d.w.}$ is Density of distilled water, w*l* is weight of liquid, $w_{d.w.}$ is weight of distilled water and $w_{e.b}$ is weight of empty gravity bottle.

3.3.5 Measurement of Ultrasonic Velocity (U)

Exploring the ultrasonic and physical properties of liquid mixtures provides valuable insights into the interactions between molecules, both within the same substance (intra-molecular) and between different substances (inter-molecular). This knowledge helps elucidate the structural organization and physicochemical behavior of these mixtures, contributing to various scientific and industrial applications. The ultrasonic interferometer is a easy and direct device to establish the ultrasonic velocity in pure liquids and binary liquid mixtures with high degree of precision. It is known for its easy operation and reliability. Measurement of ultrasonic velocity is based on accurate determination of the wavelength of sound waves in the medium. The ultrasonic interferometer (Model: F-05) from M/s. Mittal Enterprises, New Delhi, operates at 2 MHz frequency with ± 2 ms^{-1} accuracy. Its main parts include a high-frequency generator and a cell/measuring assembly, depicted in Figure 3.15.

Fig. 3.15 Ultrasonic Interferometer.

Ultrasonic waves with a known frequency are generated by an X-cut quartz crystal positioned at the bottom of the measuring cell. These waves propagate through the liquid and are reflected by a movable metallic plate positioned parallel to the crystal. Standing waves are established in the medium when the distance between the

transducer (the crystal) and the reflector plate is an integral multiple of half the wavelength of the ultrasonic waves. This phenomenon occurs due to constructive interference, where the reflected waves reinforce the incident waves, leading to areas of maximum and minimum pressure called nodes and antinodes, respectively. Reflected waves returning to the crystal surface are out of phase, causing a decrease in crystal oscillation amplitude, which generates an alternating current through the crystal. The oscillator is connected to a circuit with a quartz crystal and capacitor tuned to the crystal's frequency. Changes in the reflector's position cause variations in the current flowing through the crystal, as shown in Figure 3.16.

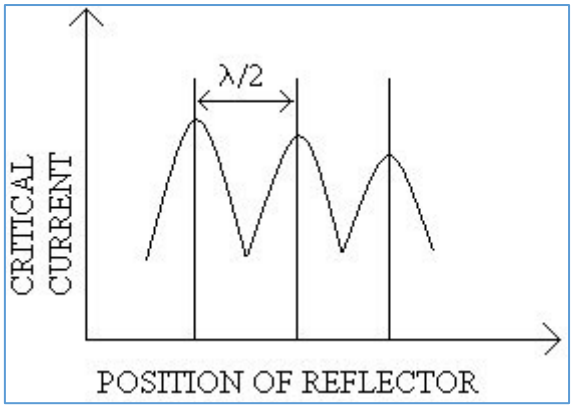

Fig. 3.16 Variation of Crystal current with Reflector position in an Interferometer.

The distance between consecutive minima and maxima represents half the wavelength in the medium. With knowledge of the crystal frequency and wavelength, we can calculate the velocity of sound in the medium. The transducer, an X-cut quartz crystal, is energized by AC energy from an RF oscillator. This transducer is a circular plate with a 1cm diameter, installed at the bottom of the measuring cell. The measuring cell is a specially designed double-walled cylindrical vessel with a capacity to hold approximately 10 ml of liquid. Water can circulate through the annular space between the two walls of the measuring cell to regulate the temperature of the liquid inside. The inner wall of the cell is corrugated to minimize reflections from the walls. A vertical electrode extends from a solid base to make electrical contact with the lower face of the crystal. A side screw is used to secure the cell in the solid base.

In fig.3.17 show the reflector is linked to a cylindrical plunger, which in turn connects to the lower end of a screw via a locking ring. A fine micro-meter screw with a precision of 0.001mm is used to control the reflector's movement, providing accurate positioning. The micrometer screw has a range of 25mm for adjustment. The quartz crystal in the

measuring cell is connected to the RF generator using a shielded cable. The cell is filled with experimental liquid. When the crystal is excited, ultrasonic waves propagate through the liquid and reflect back from the reflector, creating standing waves between the crystal and the reflector.

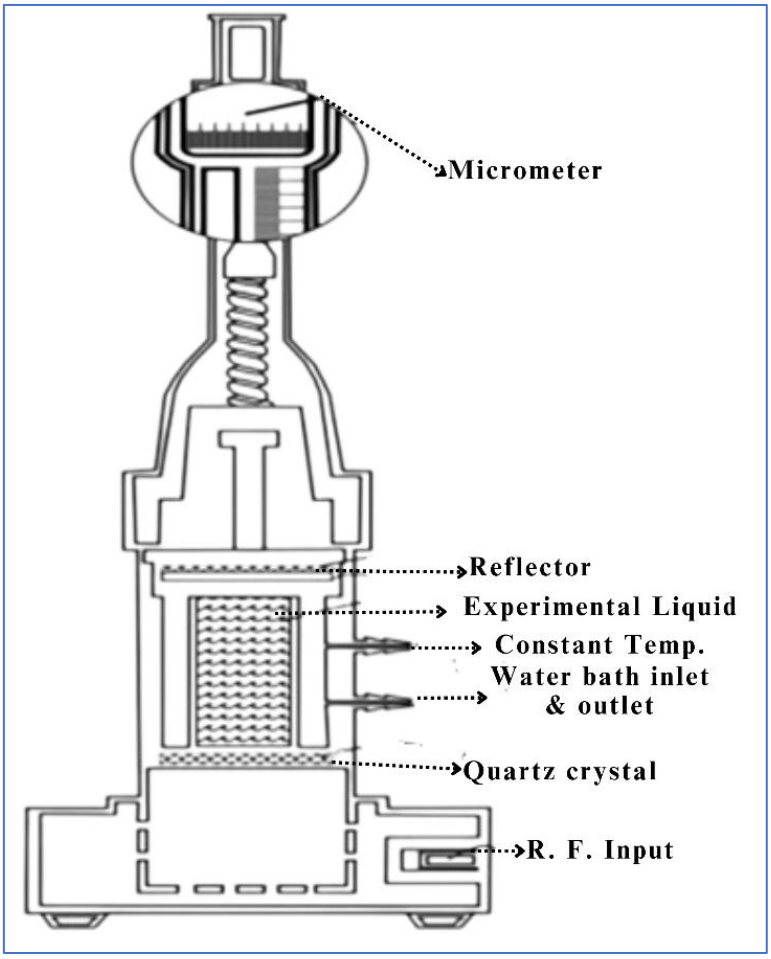

Fig. 3.17 Cross Sectional View of Liquid Cell.

The micrometer screw is adjusted upwards until the anode current in the microammeter reaches maximum deflection. The initial reading of the micrometer screw is carefully recorded. Then, the screw is rotated slowly in the same direction until ten successive maxima are allowed to pass. The reading on the micrometer screw corresponding to the tenth maxima is noted. The total distance 'd' through which the reflector shifted for 'n' maxima is determined. The wavelength 'λ' is calculated using the formula $\lambda = 2d/n$. With the known values of 'λ' and the frequency 'f' of the quartz crystal (2MHz), the velocity of sound 'U' is calculated using the following equation:

Ultrasonic velocity (U) = λ (Wavelength) × f (Frequency) (3.4)

3.3.6 Measurement of Viscosity (U)

Understanding the viscosity of binary mixtures is crucial in many industrial processes. Viscosity, among other physical properties of liquids, is vital for designing and optimizing these procedures.[7] Viscosity data for liquid mixtures helps in understanding their fundamental behavior, correlating mixture viscosities with those of pure components, and selecting appropriate physicochemical analysis methods. In industries such as chemical, food, cosmetic, and pharmaceuticals, viscosity is indispensable for hydraulic and energy transfer calculations during fluid transport. Viscometers, instruments used for measuring viscosity, estimate flow rate and applied force or work. [10-14] Rotating cylinder viscometers, for example, operate by shearing a thin liquid film between concentric containers.

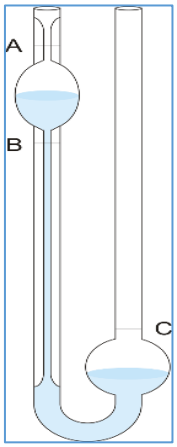

Fig. 3.18 Ostwald Viscometer.

Viscosity measurement typically employs an Ostwald viscometer, depicted in Figure 3.18. This viscometer comprises a bulb A connected to a capillary tube B, with a storage bulb C providing a constant head of liquid. The time taken (t) for the liquid to flow through the capillary is measured to determine viscosity.[9]

1. Clean the viscometer using tap water, distilled water (DW), and acetone. Hang it vertically and connect a perfect elastic cylinder with a screw pinchcock to end A for optimal cleaning.
2. Fill the viscometer with the specified amount of water until it reaches the mark. Then, draw water from end A until it surpasses the mark. Finally, let the water flow back through the tube naturally due to gravity.
3. Start the timer when the meniscus reaches mark A. Record the time when it crosses point B as t_1. Repeat this process multiple times. Perform the same steps with the liquid under test and record the time as t_2.

4. For temperature variation, submerge the Ostwald's viscometer in a steady temperature water bath at the temperature necessary for the exploratory liquid viscosity measurement.
5. Equation 3.4 can be used to determine the viscosity of an unknown liquid material.

$$\text{Viscosity of liquid } (\eta_2) = \eta_1 \times \frac{t_2}{t_1} \times \frac{\rho_2}{\rho_1} \text{ (in poise)} \quad (3.4)$$

3.4 Evaluation of Different Parameters

3.4.1 Evaluation of different dielectric/electric parameters

- **Complex Dielectric Function ε*(f)**

Impedance spectroscopy involves measuring small electrical signals to analyze a material's linear response, including electrode effects, providing insights into molecular interactions in dielectric materials [15]. Equation 3.2 determines the complex dielectric permittivity, with α = 1 yielding the real and imaginary parts [16].

$$\varepsilon'(f) = \frac{C_P}{C_0} \text{ and } \varepsilon''(f) = \frac{1}{2\pi f\, C_0 R_P} \quad (3.5)$$

Where ε' represents the real part of the complex dielectric function (dielectric constant), and ε" represents the imaginary part (dielectric loss). The relative dielectric loss of the material can be calculated as [16].

$$\tan\delta = \frac{\varepsilon''}{\varepsilon'} \quad (3.6)$$

where tanδ is the dielectric loss tangent of the material.

- **Complex Electric Modulus M*(f)**

The frequency-dependent values of M*(f) are determined using the relation [17,18].

$$M^*(f) = M' + jM'' = \frac{\varepsilon'}{\varepsilon'^2 + \varepsilon''^2} + j\frac{\varepsilon''}{\varepsilon'^2 + \varepsilon''^2} \quad (3.7)$$

Where ε′ and ε′′ shows the real and imaginary part of permittivity. The inverse of the dielectric function M is denoted by the symbol $M^*(f) = \frac{1}{\varepsilon^*(f)}$.

The frequency fσ corresponding to this peak is related to the most probable ionic conductivity relaxation time is given by

$$\tau_\sigma = \frac{1}{2\pi f_\sigma} \quad (3.8)$$

- **Complex Electrical Conductivity σ * (f)**

The frequency-dependent complex electric conductivity (σ*(f)) for the liquid mixtures were determined by the following equation:[18]

$$\sigma^*(f) = \sigma' + j\sigma'' = \omega\varepsilon_0\varepsilon'' + j\omega\varepsilon_0\varepsilon' \quad (3.9)$$

Where ω is the angular frequency and ε_0 is the permittivity of the free space and ε′ is real part of permittivity and ε″ is imaginary part of permittivity respectively. The σ′ versus frequency spectra usually exhibit frequency independent plateau which corresponds to ionic or dc electrical conductivity σ_{dc}.

- **Complex Impedance Z*(f)**

The complex impedance spectra $Z^*(f)$ of the materials can be determined using equation.[18]

$$Z^*(f) = Z' - jZ'' = \frac{\varepsilon''}{\omega C_0(\varepsilon'^2+\varepsilon''^2)} - j\frac{\varepsilon'}{\omega C_0(\varepsilon'^2+\varepsilon''^2)} \quad (3.10)$$

where ω represents angular frequency, C_0 denotes the electric capacity of the empty measuring cell, ε' is the real part of permittivity, and ε" is the imaginary part of permittivity. Complex impedance plots (Z″ vs Z′) are frequently used to distinguish between bulk material and electrode surface polarization phenomena. A notable characteristic of dielectrics with DC conductivity is the discontinuity observed at the electrode/dielectric interface, which exhibits distinct polarization properties compared to the bulk dielectric material.

3.4.2 Evaluation of Thickness of ion build up, Ion Mobility, Mobile Ion Concentrations and Ion Diffusivity

Klein [19] introduced a model enabling the determination of mobile ion concentration and ion mobility using measured complex dielectric data on single-ion conductors. The calculation of Debye Length (λ_D), ion mobility (μ), mobile ion concentration (P_0), and ion diffusivity (D) within the concentration range ($0.0 \leq X_A \leq 1.0$) was conducted utilizing the model equation proposed by Klein et al. [19] Determining the thickness of the ions buildup at the electrode surface is given by:

$$\lambda_D = \frac{g}{2M} \quad (3.11)$$

Where, the gap between the electrodes (g), the thickness of the layer where ions gather on the electrode surface (λ_D), and a ratio $M = \frac{\tau_{EP}}{\tau_\sigma}$. τ_{EP} is Electrode polarization relaxation time and is obtained by ε" spectra and τ_σ Ionic conduction relaxation time and is obtained from M" spectra.

Ion mobility is a quantity in which large fraction of the total ion concentration is bound up in ion pairs or clusters [19]. Calculations of ion mobility was calculated using by

$$\mu = \frac{9g^2}{4kTM\tau_{EP}} \tag{3.12}$$

Where q is electron charge, k is Boltzmann constant and T is Temperature, respectively. The mobile ion concentration can vary with temperature in a complex manner [20]. Calculating concentrations of mobile ions (P_0) and diffusivity (D) was done using the ion mobility.

$$P_0 = \frac{\sigma_{dc}}{q\mu} \tag{3.13}$$

$$D = \frac{\mu KT}{q} \tag{3.14}$$

In the given equation, where μ represents ion mobility, K is the Boltzmann constant, T is the absolute temperature, and q denotes the charge of the electron.

3.4.3 Evaluation of Kirkwood Correlation Parameters and Bruggeman Parameter

Some valuable insights into dipole-dipole correlation and the orientation of electric dipoles in two polar liquids can be gained using the Kirkwood correlation factor (g). The expression for the pure liquids is as follows [21-24]

$$\left(\frac{4\pi N\mu^2\rho}{9KTM}\right) g = \frac{(\varepsilon_0-\varepsilon_\infty)(2\varepsilon_0+\varepsilon_\infty)}{\varepsilon_0(\varepsilon_\infty+2)^2} \tag{3.15}$$

The modified Kirkwood equation is used to determine the effective averaged angular Kirkwood correlation factor (g^{eff}) of the two constituent molecules of the mixture of two polar liquids. This modified Kirkwood equation is given below: [25-27]

$$\frac{4\pi N}{9KT}\left(\frac{\mu_1^2\rho_1}{M_1}X_1 + \frac{\mu_2^2\rho_2}{M_2}X_2\right) g^{eff} = \frac{(\varepsilon_{0m}-\varepsilon_{\infty m})(2\varepsilon_{0m}+\varepsilon_{\infty m})}{\varepsilon_{0m}(\varepsilon_{\infty m}+2)^2} \tag{3.16}$$

The corrective correlation factor (g^F) which influences the angular correlation factors of pristine substances 1 and 2 is represented as:[28]

$$\frac{4\pi N}{9KT}\left(\frac{\mu_1^2\rho_1 g_1}{M_1}X_1 + \frac{\mu_2^2\rho_2 g_2}{M_2}X_2\right) g^F = \frac{(\varepsilon_{0m}-\varepsilon_{\infty m})(2\varepsilon_{0m}+\varepsilon_{\infty m})}{\varepsilon_{0m}(\varepsilon_{\infty m}+2)^2} \tag{3.17}$$

Here, N is Avogadro's number, μ is the dipole moment of the molecules forming the liquid, ρ is density of the liquid at temperature T in the kelvin scale. M is the molecular weight, ε_∞ and ε_0 are of the high frequency limiting dielectric constant and the static permittivity. The suffixes 1, 2 and m represent liquid 1(n-Hexanol, n-Octanol), liquid 2 (DMF) and mixture, respectively.

The Bruggeman parameter (f_B), provides information on the interaction that occurs between the participating components of the mixture [21-24,29]. According to

Bruggeman ε_{01}, ε_{02} and ε_{0m} are related to volume fraction of solute by the following equation.

$$f_B = \left(\frac{\varepsilon_{0m}-\varepsilon_{02}}{\varepsilon_{01}-\varepsilon_{02}}\right)\left(\frac{\varepsilon_{01}}{\varepsilon_{0m}}\right)^{\frac{1}{3}} = (1-\Phi_2) \quad (3.18)$$

In equation 3.18, Φ_2 represents the volume fraction of liquid 2 (DMF), where ε_{01}, ε_{02}, and ε_{0m} are the static dielectric constants of liquid 1 (n-Hexanol, n-Octanol), liquid 2 (DMF), and the binary mixture, respectively.

3.4.4 Evaluation of Microwave Dielectric Relaxation Parameters

The microwave dielectric relaxation properties, like the relaxation time (τ_0) and dielectric strength ($\Delta\varepsilon$), are determined through fitting experimental data to different models (HNHN/CC/CD/Debye). These models consider asymmetry and broadening in the dielectric relaxation using the CNLS method [30]. One such widely used model is the Havriliak-Negami (HN) equation [31].

$$\varepsilon(\omega) = \varepsilon_\infty + \frac{\Delta\varepsilon}{[1+(i\omega\tau)^\alpha]^\beta} \quad (3.19)$$

In this study, the complex permittivity at angular frequency ω, is analyzed. The difference between the static dielectric constant (ε_0) and the optical dielectric constant ($\varepsilon\infty$) is defined as the dielectric strength ($\Delta\varepsilon$), while τ represents the relaxation time of the mixture concentration. Two shape parameters, α and β, play a crucial role in selecting dielectric relaxation models. Specifically, the Cole-Davidson (CD) model, characterized by α = 1, and the Cole-Cole (CC) model, characterized by β = 1 and Debye Model characterized by α = β = 1 represent symmetrical and asymmetric relaxation curves, respectively.

3.4.5 Excess Dielectric Parameters

The excess parameters related with (ε_0) and (τ_0) provide important insights into the mixing behavior of binary liquid mixtures interaction. The excess static dielectric constant $(\varepsilon_0)^E$ and excess inverse relaxation time $(1/\tau)^E$ are computed using the following relations. [32-34]

$$(\varepsilon_0)^E = (\varepsilon_0-\varepsilon_\infty)_m - [(\varepsilon_0-\varepsilon_\infty)_1 X_1 + (\varepsilon_0-\varepsilon_\infty)_2 X_2] \quad (3.20)$$

$$\left(\frac{1}{\tau_0}\right)^E = \left(\frac{1}{\tau_0}\right)_m - \left[\left(\frac{1}{\tau_0}\right)_1 X_1 + \left(\frac{1}{\tau_0}\right)_2 X_2\right] \quad (3.21)$$

where 'X' is mole fraction and suffixes 'm', '1', '2' represent mixture, liquid 1 (n-Hexanol, n-Octanol) liquid 2 (DMF) respectively. Excess static dielectric constant $(\varepsilon_0)^E$,

excess inverse relaxation time $(1/\tau_0)^E$ data fitted in R. K. Polynomial. R. K. Polynomial equation given by [34]

$$(A)^E = X_1X_2\sum_i^n a_i \cdot (X_2 - X_1)^i \quad (3.22)$$

Where 'a_i' stands for fitting parameters, X_1 and X_2 have usual meanings, n is the degree of polynomial expansion.

3.4.6 Evaluation of Thermodynamic Parameters of Microwave Dielectric Relaxation

Dielectric relaxation process can be understood of as the dipole rotating between two equilibrium positions separated by a potential barrier. The dielectric relaxation time (τ_0), depends on the height of the potential barrier, a constant that changes with temperature, and the average time it takes for an excited molecule to move from one equilibrium position to the other [35]. According to Eyring dielectric relaxation is related to the chemical rate theory [35-37].

$$\tau_0 = \left(\frac{h}{kT}\right)\exp\left(\frac{\Delta Fe}{RT}\right) \quad (3.23)$$

$$\Delta F_e = RT\ln\left(\frac{\tau_0 KT}{h}\right) \quad (3.24)$$

The change in activation energy is also expressed as

$$\Delta F_e = \Delta He - T\Delta s \quad (3.25)$$

In these various thermodynamic parameters are discussed in relation to a mixture of DMF (Dimethylformamide) and (n-Hexanol, n-Octanol). These parameters include τ_0 (dipolar relaxation time), h (Planck's constant), R (universal gas constant), K (Boltzmann's constant), and T (absolute temperature in Kelvin).

3.4.7 Evaluation of Microwave heating parameters

The microwave frequency 2.45 GHz have been specified for industrial use in order to avoid from possible interference with frequencies used for telecommunications, the military, and navigation applications. The microwave heating parameters like penetration depth (d_p), power reflected (P_r) and power transmitted (P_t) are determined from the observed values of dielectric constant (ε') and dielectric loss (ε'') at 2.45 GHz frequency using following equations [38].

$$P_r = \left(\frac{\sqrt{\varepsilon'}-1}{\sqrt{\varepsilon''}+1}\right)^2 \quad (3.26)$$

$$P_t = \left[100 - \left(\frac{\sqrt{\varepsilon'}-1}{\sqrt{\varepsilon''}+1}\right)^2\right] \quad (3.27)$$

$$d_P = \frac{\lambda_0}{2\pi}\frac{\sqrt{\varepsilon'}}{\varepsilon''} \quad (3.28)$$

Where $\lambda_0 = \frac{c}{f}$. c is the speed of light in free space (3×10^8 m/s) and f is the microwave frequency (Hz).

3.4.8 Evaluation of Refractometric parameters

Values of the molar volume (V_m) has been determined from the experimentally determined density (ρ) of pure substances and its mixtures.[39]

$$V_m = \frac{(X_1M_1 + X_2M_2)}{\rho} \quad (3.29)$$

In this equation, X_1 and X_2 are the mole fractions of liquid 1 (n-hexanol, n-Octanol) and liquid 2 (DMF), M_1 and M_2 are their molecular masses, and ρ is their density of the solutions.

Information regarding the presence of certain intermolecular interactions in the binary liquid mixture can be obtained by the molar refraction (Rm) [40]

$$R_m = \left(\frac{n^2-1}{n^2+2}\right)V_m \quad (3.30)$$

where n is the refractive index of the liquid and $V_m = M/\rho$ is molecular volume. M and ρ is the molecular weight and the density of the pure liquids respectively.

The atomic polarization (P_A) is calculated from the refractive indices (n) of pure substances and mixtures by equation.[41]

$$P_A = 1.05\, n^2 \quad (3.31)$$

Where, n is refractive index of the liquid.

Lorentz Formula is used to calculate the molecular polarizability (α) of the liquid.[42]

$$\alpha = \frac{3V_m}{4\pi N}\left(\frac{n^2-1}{n^2+2}\right) \quad (3.32)$$

Where N is the Avogadro's constant and V_m is molar volume.

Using the values for the refractive index, we have calculated the molecular radii of pure liquids theoretically.[43]

$$r = \left[\left\{\left(\frac{3}{4\pi N}\right)\left(\frac{n^2-1}{n^2+2}\right)\right\}V_m\right]^{\frac{1}{3}} \quad (3.33)$$

The well-known Buchler- Hirschfelder-Curtiss equation of state, which is provided as following, can be used to calculate the internal pressures of binary liquid mixtures.[44]

$$P_{int} = \frac{2^{\frac{1}{6}}RT}{2^{\frac{1}{6}}V_m - 2rN^{\frac{1}{3}}V_m^{\frac{2}{3}}} \quad (3.34)$$

In eq.6 in variables T, Vm, r, N, and R represent the absolute temperature, molar volume, molecular radius, Avogadro's constant and universal gas constant, respectively.

- **Excess Parameters of refractometric of binary liquid mixtures**

The excess function provides an idea of the amount of deviation of the given liquid mixtures from ideality. Understanding the nature of molecular campaigning and intermolecular interactions in heteromolecular is fundamentally dependent on excess properties. In the present study, we have calculated excess refractive index (Δn), excess molar volume (ΔV_m), excess reduce free volume ($\Delta(V_m/R_m)$), excess atomic polarization (ΔP_A), excess molecular radii (Δr) and excess internal pressure (ΔP_{int}) of the binary mixtures. They are evaluated from the below equations. [39,43-44]

$$\Delta n = n_m - (n_1X_1 + n_2X_2) \tag{3.35}$$

$$\Delta V_m = V_m - \left(V_{m_1}X_1 + V_{m2}X_2\right) \tag{3.36}$$

$$\frac{\Delta V_m}{\Delta R_m} = \left(\frac{V_m}{R_m}\right) - \left[\left(\frac{V_{m1}}{R_{m1}}\right)X_i + \left(\frac{V_{m2}}{R_{m2}}\right)X_2\right] \tag{3.37}$$

$$\Delta P_{A_m} = \Delta P_{A_m} - \left(\Delta P_{A_1}X_1 + \Delta P_{A_2}X_2\right) \tag{3.38}$$

$$\Delta r = r_m - (r_1X_1 + r_2X_2) \tag{3.39}$$

$$\Delta P_{int} = P_{int\,m} - (P_{int\,1}X_1 + P_{int\,2}X_2) \tag{3.40}$$

Where, X the mole fraction of binary mixtures. The subscripts m, 1, and 2 denotes mixtures of molecular species liquid 1 (n-Hexanol, n-Octanol) and liquid 2 (DMF) respectively. The deviation (Δn), (ΔV_m), (ΔP_{Am}), ($\Delta V_m/\Delta R_m$), (Δr) and (ΔP_{int}) have been fitted to the using Redlich-Kister polynomial Eq. 3.22. The standard deviations (σ) were calculated using the relation. [39]

$$\sigma = \left[\frac{\sum(A^E_{experimental} - A^E_{calculated})^2}{N-n}\right]^{\frac{1}{2}} \tag{3.41}$$

where n is the number of coefficients and N is the number of experimental data points.

3.4.9 Evaluation of Acoustic parameters

- **Ultrasonic Velocity (U)**

The ultrasonic velocity in a liquid can be determined using interferometric methods by measuring the wavelength (λ) of the ultrasonic wave in the liquid mixture. This velocity is often related to the molecular structure of the liquid's constituents and its thermodynamic properties. The formula used to calculate ultrasonic velocity typically involves dividing the wavelength of the ultrasonic wave by the time it takes for the

wave to travel a known distance through the liquid. This formula can be expressed as: [45]

Ultrasonic velocity (U) = Frequency (F) × Wavelength (λ) (3.42)

Where U is the velocity of the ultrasonic wave, F is the frequency of the ultrasonic generator (2.0094 Hz), λ is the wavelength of the ultrasonic wave.

- **Adiabatic Compressibility (β)**

Adiabatic compressibility (β) also known as isentropic compressibility, represents the relative volume change of a fluid mixture under pressure variation without heat exchange. This property offers insights into the behavior of the medium. The relationship between adiabatic compressibility, ultrasonic velocity, and density of the mixture is described by an equation.[46]

$$\beta = \frac{1}{U^2 \rho} \quad (3.43)$$

- **Intermolecular Free Length (L_f)**

The adiabatic compressibility of a fluid can be related to the intermolecular free length, which defines the distance between neighboring atoms' surfaces. This relationship can be expressed using the following equation:[47]

$$L_f = k \cdot \beta^{\left(\frac{1}{2}\right)} \quad (3.44)$$

where K is called the Jacobson constant and is given by K = (93.875 + 0.375 T) x 10^{-8}, where T is the temperature in Kelvin.

- **Acoustic Impedance (Z)**

Acoustic impedance (Z) is the measure of resistance that a fluid mixture presents to the acoustic flow, resulting in acoustical pressure associated with the structure. It is calculated using the following equation: [48]

$$z = \rho u \quad (3.45)$$

Where ρ is density and u is ultrasonic velocity.

- **Molar Sound Velocity (R)**

Molar sound velocity is also recognized as Rao's constant and it is an additive property. R is a relation between ultrasonic velocity and molar volume, which is given by [49]

$$R = \left(\frac{M}{\rho}\right)(u)^{1/3} \quad (3.46)$$

Where M is molar mass, ρ is density and u is ultrasonic velocity respectively.

- **Molar compressibility (B)**

Molar compressibility is also known as Wada's constant, which is dependent on adiabatic compressibility and density is given by [49]

$$W = \left(\frac{M}{\rho}\right)(\beta)^{-1/7} \quad (3.47)$$

- **Molar Volume (Vm)**

Molar volume is an important parameter which is used to calculate other physical parameters and also indicates the nature of interaction. The measured density (ρ) of samples was used to find the molar volume (Vm) by equation [50]

$$V_m = \frac{x_1 m_1}{\rho_1} + \frac{x_2 m_2}{\rho_2} \quad (3.48)$$

Where X and M are the mole fraction and molecular weight, respectively. The suffix 1, 2 and m represent liquid 1, liquid 2 and mixture, respectively.

- **Relaxation Time (τ)**

Relaxation time is the duration it takes for molecules to go back to their original positions after being moved by an external force. It's calculated using a specific formula. [51]

$$\tau = \frac{4}{3}\eta\beta \quad (3.49)$$

Where η is viscosity and β is adiabatic compressibility.

- **Free Volume (V_F)**

Free volume can be determined through dimensional analysis utilizing experimentally measurable parameters such as ultrasonic velocity and viscosity. The formula for calculating free volume can be expressed as:[52]

$$V_F = \left(\frac{Me_{ff}U}{K\eta}\right)^{\frac{3}{2}} \quad (3.50)$$

Where Meff is molar mass and U is ultrasonic velocity, K is called the Jacobson constant and is given by K = (93.875 + 0.375 T) x 10^{-8} and η is viscosity.

- **surface tension (σ)**

The surface tension from Flory theory has been used to evaluate ultrasonic velocity of mixture, with the help of relation [53]

$$\sigma = 6.4 \times 10^{-10}\,\rho(u)^{3/2} \quad (3.51)$$

- **Thermal conductivity (K)**

The determination of thermal conductivity k is important for evaluating the suitability of a fluid or nanofluid for use in various heat transfer systems [49]

$$k = 2.8\, u \left(\frac{N_A}{V}\right)^{2/3} K_B \qquad (3.52)$$

Where N_A is the Avogadro number, V is the molar volume of the liquid and K_B is the Boltzmann's constant.

References

[1] D. H. Gadani, A. D. Vyas, V. A. Rana, S. P. Bhatnagar, A. N. Prajapati, Dielectric spectroscopy of dry and wet soils in frequency region from 20 Hz to 20 GHz, Solid State Phenom. 209 (2014) 23-26.

[2] N. S. Shah, P. S. Shah, V. A. Rana, Dielectric and electrical properties of coconut water and distilled water in the frequency range 20 Hz to 2 MHz at different temperatures, Ionics 21 (2015) 3217-3222.

[3] S. Manual, Operation and Service Manual, ReVision, (2015) 1-29.

[4] SPEAG, Dielectric Assessment Kit (DAK) Professional Handbook, Version 2.2 (2017).

[5] D. K. Barot, Dielectric properties of solutions of 1-Butyl-3-Methyl Imidazolium chloride in polar solvents, Ph.D. Thesis, Gujarat University. (2019).

[6] H. P. Vankar, V. A. Rana, S. Dey, H. D. Patel, V. K. Jain, Molecular interaction in binary mixtures of 3-Bromoanisole and methanol: A microwave dielectric relaxation spectroscopy and molecular dynamic simulation study, J. Mol. Liq. 325 (2021) 115186.

[7] A. Hayyana, F. S. Mjalli, I. M. AlNashef, T. Al-Wahaibi, Y. M. Al-Wahaibi, M. A. Hashim, Fruit sugar-based deep eutectic solvents and their physical properties, Thermochim. Acta 541 (2012) 70-75.

[8] A. Hayyan, F. S. Mjalli, I. M. AlNashef, Y. M. Al-Wahaibi, T. Al-Wahaibi, M. A. Hashim, Glucose-based deep eutectic solvents: Physical properties, J. Mol. Liq. 178 (2013) 137-141.

[9] I. Saxena, R. N. Pathak, V. Kumar, R Devi, Introduction of ultrasonic interferometer and experimental techniques for determination of ultrasonic velocity, density, viscosity and various thermodynamic parameters, Int. J. Appl. Res. 1 (2015) 562-569.

[10] V. Herraez, R. Belda, O. Diez, M. Herraez, An equation for the correlation of viscosities of binary mixtures, J. Solut. Chem. 37 (2008) 233-248.

[11] E. L. Heric, J. G. Brewer, Viscosity of some binary liquid nonelectrolyte mixtures, J. Chem. Eng. Data 12 (1967) 574-583.

[12] B. Irving, Viscosities of binary liquid mixtures: A survey of mixture equations, NEL Rep. No. 630 (1977).

[13] S. W. Benson, Methods for the estimation of thermochemical data, Thermochem. Kinet. 2nd Ed.; Wiley, New York (1976)19-77.

[14] J. A. Dean, Handbook of organic chemistry, McGraw-Hill, New York (1987).

[15] H. Mehta, R. Narayan, G. Aithal, S. Pandiyan, P. Bhat, S. Dengale, S. Garg, Molecular simulation driven experiment for formulation of fixed dose combination of Darunavir and Ritonavir as anti-HIV nanosuspension, J. Mol. Liq. 293 (2019) 111469.

[16] Technologies, 16452A Liquid Test Fixture Operation and Service Manual (2017).

[17] R. J. Sengwa, S. Sankhla, Characterization of ionic conduction and electrode polarization relaxation processes in ethylene glycol oligomers, Polym. Bull. 60 (2008) 689-700.

[18] R. J. Sengwa, S. Choudhary, P. Dhatarwal, Characterization of relaxation processes over static permittivity frequency regime and compliance of the Stokes-Einstein-Nernst relation in propylene carbonate, J. Mol. Liq. 225 (2017) 42-49.

[19] R. J. Klein, S. Zhang, S. Dou, B. H. Jones, R. H. Colby, J. Runt, Modeling electrode polarization in dielectric spectroscopy: Ion mobility and mobile ion concentration of single-ion polymer electrolytes, J. Chem. Phys. 124 (2006)144903.

[20] B. Haldar, R. M. Singru, K. K. Maurya, S. Chandra, Temperature dependence of positron-annihilation lifetime, free volume, conductivity, ionic mobility, and number of charge carriers in a polymer electrolyte polyethylene oxide complexed with NH4ClO4, Phys. Rev. B 54 (1996) 7143.

[21] A. N. Prajapati, V. A. Rana, A. D. Vyas, S. P. Bhatnagar, Study of heterogeneous interaction through dielectric properties of binary mixtures of fluorobenzene with methanol, Solid State Phenom. 209 (2011) 23-26.

[22] A. N. Prajapati, S. P. Patel, V. A. Rana, Study of short range and long range molecular interactions in binary liquid mixtures of N, N-dimethylformamide (DMF) and 1-propanol, J. Mol. Liq. 354 (2022)118832.

[23] R. J. Sengwa, M. Madhvi, S. Sankhla, S. Sharma, Characterization of heterogeneous interaction behavior in ternary mixtures by a dielectric analysis: equi-molar H-bonded binary polar mixtures in aqueous solutions, J. Solut. Chem. 35 (2006) 1037-1055.

[24] R. J. Sengwa, S. Choudhary, V. Khatri, Microwave dielectric spectra and molecular relaxation in formamide–N, N-dimethylformamide binary mixtures, Spectrochim. Acta A 82 (2011) 279-282.

[25] S. P. Patel, A. N. Prajapati, Dielectric properties of binary liquid mixtures-Winkelmann-Quitzsch approach, AIP Conf. Proc. 2220 (2020) 040018.

[26] T. M. Mohan, S. S. Sastry, V. R. K. Murthy, Thermodynamic, dielectric and conformational studies on hydrogen bonded binary mixtures of propan-1-ol with methyl benzoate and ethyl benzoate, J. Solut. Chem. 40 (2011) 131-146.

[27] M. Rabinovitz, A. Pines, Hindered internal rotation and dimerization of N, N-dimethylformamide in carbon tetrachloride, J. Am. Chem. Soc. 91 (1969) 1585-1589.

[28] A. N. Prajapati, V. A. Rana, A. D. Vyas, Dielectric dispersion studies of mixtures of aniline and benzonitrile in benzene solutions, J. Mol. Liq. 144 (2009)1-4.

[29] K. Ramachandran, P. Sivagurunathan, K. Dharmalingam, S. C. Mehrotra, Dielectric relaxation study of amide-alcohol mixtures by using time domain reflectometry, Acta Phys.-Chim. Sin. 23 (2007)1508-1515.

[30] J. MacDonald, LEVM/LEVMW manual-CNLS (Complex nonlinear least squares) immittance, inversion, and simulation fitting programs for WINDOWS and MS-DOS, version 20.09 (2013).

[31] S. Havriliak, S. Negami, A complex plane analysis of α-dispersions in some polymer systems, J. Polym. Sci. Part C: Polym. Symp. 14 (1966) 99-117.

[32] T. P. Iglesias, J. L. Legido, S. M. Pereira, B. De Cominges, M. P. Andrade, Relative permittivities and refractive indices on mixing for (n-hexane + 1-pentanol, or 1-hexanol, or 1-heptanol) at T = 298.15 K, J. Chem. Thermodyn. 32 (2000) 923-930.

[33] S. C. Mehrotra, J. E. Boggs, Effect of collision-induced phase shifts on the linewidths and line shifts of rotational spectral lines, J. Chem. Phys. 66 (1977) 5306-5312.

[34] A. C. Kumbharkhane, S. M. Puranik, S. C. Mehrotra, Dielectric relaxation studies of aqueous N, N-dimethylformamide using a picosecond time domain technique, J. Solut. Chem. 22 (1993) 219-229.

[35] M. T. Hosamani, N. H. Ayachit, D. K. Deshpande, Activation energy (ΔG*), enthalpy (ΔH*), and entropy (ΔS*) of some indoles and certain of their binary mixtures, J. Therm. Anal. Calorim. 107 (2012) 1301-1306.

[36] S. S. Birajdar, A. C. Kumbharkhane, S. N. Hallale, P. G. Hudge, D. B. Suryawanshi, Thermodynamic and dielectric properties of cyclohexanol-xylene binary mixtures using dielectric spectroscopy, Polycycl. Aromat. Compd. 43 (2023)1619-1627.

[37] C. V. Maridevarmath, G. H. Malimath, Studies on the effect of temperature on dielectric relaxation, activation energy (ΔG*), enthalpy (ΔH*), entropy (ΔS*) and molecular interactions of some anilines, phenol and their binary mixtures using X-band microwave bench, J. Chem. Thermodyn. 144 (2020) 106068.

[38] V. A. Rana, T. R. Pandit, Microwave dielectric relaxation spectroscopy of paracetamol and its aqueous solutions, J. Mol. Liq. 314 (2020) 113673.

[39] A. N. Prajapati, V. A. Rana, A. D. Vyas, D. H. Gadani, Optical and volumetric study of molecular interactions in binary mixtures of 1-propanol (1-PrOH) and fluorobenzene (FB), J. Int. Acad. Phys. Sci. 16 (2012) 387-398.

[40] D. Dragoescu, Refractive indices and their related properties for several binary mixtures containing cyclic ketones and chloroalkanes, J. Mol. Liq. 209 (2015) 713-722.

[41] A. N. Prajapati, C. S. Limberkar, Study of concentration dependent physico-chemical properties of 1-Propanol, Benzonitrile and their binary mixtures, Int. J. of advance. in elect. and comp. eng. 3 (2014) 297-301.

[42] V. A. Rana, N. S. Shah, K. N. Shah, H. P. Vankar, Dielectric spectroscopy and molecular dynamic simulation study of binary mixtures of benzaldehyde and methanol at 303.15 K, J. Mol. Liq. 369 (2023)120829.

[43] A. Ali, M. Tariq, Deviations in refractive index parameters and applicability of mixing rules in binary mixtures of benzene + 1,2-dichloroethane at different temperatures, Chem. Eng. Commun. 195 (2007) 43-56.

[44] R. Srivastava, V. K. Pandeya, A. Awasthi, A. Awasthi, Internal pressure and optical properties of binary mixture of formamide with dimethylaminoethanol and diethylaminoethanol at different temperatures, Indian J. Pure Appl. Phys. 57 (2019) 879-884.

[45] N. Mohanty, Molecular interaction study of DI-n-Butyl phthalate (DBT) with some polar and non-polar liquids using ultrasonic interferometer at different frequencies and at constant temperature, Ph.D. Thesis, Ravenshaw University. (2013).

[46] M. J. Moran, H. N. Shapiro, D. D. Boettner, M. B. Bailey, Fundamentals of engineering thermodynamics, John Wiley & Sons (2010).

[47] B. Jacobson, Ultrasonic velocity in liquids and liquid mixtures, J. Chem. Phys. 20 (1952) 927-928.

[48] S. k. Fakruddin, Ch. Srinivas, N. Kolla, Study of ultrasonic parameters in binary liquid mixture containing quinoline and o-xylene at different temperatures, J. Chem. Pharm. Res. 4 (2012) 3606-3609.

[49] M. Saraswat, R. J. Sengwa, Multiphysics experimental approaches for insight into the hydrogen bonded structures of ethylene glycol and glycerol mixtures toward green solvent technology, Indian J Pure Appl Phys, 61 (2023) 217-238.

[50] M. I. Aralaguppi, C. V. Jadar, T. M. Aminabhavi, Density, viscosity, refractive index, and speed of sound in binary mixtures of acrylonitrile with methanol, ethanol, propan-1-ol, butan-1-ol, pentan-1-ol, hexan-1-ol, heptan-1-ol, and butan-2-ol, J. Chem. Eng. Data 44 (1999) 216-221.

[51] B. Hinner, M. Tempel, E. Sackmann, K. Kroy, E. Frey, Entanglement, elasticity, and viscous relaxation of actin solutions, Phys. Rev. Lett. 81 (1998) 2614.

[52] N. Prasad, Excess free volume and internal pressure of binary solutions of N, N-dimethyl aniline and halomethanes, J. Pure Appl. Ultrason. 25 (2003) 25-30.

[53] S. Nithiyanantham, Ultrasonic velocity models in liquids (micro-and nanofluids): theoretical validations, Int Nano Lett, 9 (2019) 89–97.